Theoretical prediction of chiral 3D hybrid organic-inorganic perovskites

Long, Guankui; Zhou, Yecheng; Zhang, Mingtao; Sabatini, Randy; Rasmita, Abdullah; Huang, Li; Lakhwani, Girish; Gao, Weibo

2019

https://hdl.handle.net/10356/142868

https://doi.org/10.1002/adma.201807628

Theoretical prediction of chiral three-dimensional hybrid organic-inorganic perovskites

Guankui Long*, Yecheng Zhou, Mingtao Zhang, Randy Sabatini, Abdullah Rasmita, Li Huang, Girish Lakhwani, Weibo Gao*

Dr. G. Long, Mr. A. Rasmita, Prof. W. Gao
Division of Physics and Applied Physics, School of Physical and Mathematical Sciences, Nanyang Technological University, Singapore, 637371, Singapore
Dr. Y. Zhou, Prof. L. Huang
Department of Physics, Southern University of Science and Technology (SUSTech), No. 1088, Xueyuan Rd, Shenzhen 518055, Guangdong, P. R. China
Prof. M. Zhang
College of Chemistry, Nankai University, Tianjin, 300071, China
Dr. R. Sabatini, Dr. G. Lakhwani
ARC Centre of Excellence in Exciton Science, School of Chemistry, The University of Sydney, NSW 2006, Australia
Prof. W. Gao
MajuLab, CNRS-Université de Nice-NUS-NTU International Joint Research Unit UMI 3654, Singapore
Prof. W. Gao
The Photonics Institute and Centre for Disruptive Photonic Technologies, Nanyang Technological University, Singapore 637371, Singapore

Hybrid organic-inorganic perovskites (HOIPs), in particular 3D HOIPs, have demonstrated remarkable properties, including ultra-long charge-carrier diffusion lengths, high dielectric constants, low trap densities, tunable absorption and emission wavelengths, strong spin-orbit coupling, and large Rashba splitting. These superior properties have generated intensive research interest in HOIPs for high-performance optoelectronics and spintronics. Here, we demonstrate 3D hybrid organic-inorganic perovskites that implant chirality through introducing the chiral methylammonium cation. Based on structural optimization, phonon spectra, formation energy and *ab initio* molecular dynamics simulations, we found that the chirality of the chiral cations can be successfully transferred to the framework of 3D HOIPs, and the

1

resulting 3D chiral HOIPs are both kinetically and thermodynamically stable. Combining chirality with the impressive optical, electrical and spintronic properties of 3D perovskites, 3D chiral perovskites would be of great interest to the field of piezoelectricity, thermoelectricity, ferroelectricity, topological quantum optics, circularly polarized optoelectronics and spintronics.

Chirality is a universal phenomenon in nature and the carrier for biological recognition and replication. For example, all twenty natural α-amino acids exhibit L-configuration except glycine, while the natural saccharides and saccharide units in cellulose, starch and deoxyribonucleic acid (DNA) exhibit D-configuration. Furthermore, novel chiral functional materials can also be employed to exploit the intrinsic non-centrosymmetric properties, including optical rotation, circular dichroism, second-harmonic generation, piezoelectricity, pyroelectricity and ferroelectricity.[1] However, for practical application in the fields of electronics, photonics and spintronics, the desired chiral material should combine low production cost (*e.g.*, low-temperature solution-processability) with impressive optical, electrical, and spintronic properties.

Hybrid organic-inorganic perovskites (HOIPs), especially 3D HOIPs have demonstrated remarkable properties, such as ultra-long charge-carrier diffusion lengths,[2] high dielectric constants,[3] low trap densities,[4] tunable absorption and emission wavelengths,[5] strong spin-orbit coupling,[6] ferroic ionic coupling[7] and large Rashba splitting.[8] This has prompted intensive research in HOIPs for high-performance optoelectronics and spintronics including in photovoltaics,[9] light-emitting diodes,[10] lasers,[5, 11] photodetectors[12] and magneto-resistance devices.[13]

Most importantly, the flexible crystal structure and ionic composition of HOIPs offer a key lever to control the structure-property relationship through rational material design:

specifically, HOIPs allow the incorporation of chiral organic ligands. In 2003, Billing *et al.* reported the synthesis of the one-dimensional (1D) chiral HOIP single crystals, which incorporated chiral ligands,[14] and also the two-dimensional (2D) chiral HOIP single crystals later in 2006.[15] Recently, we have extended this to reduced-dimensional chiral perovskites (a.k.a. *Ruddlesden-Popper* or quasi-2D perovskite) through combined strategies of chirality transfer and energy funneling.[16] Both spin-polarized absorption and spin-polarized photoluminescence were observed in these reduced-dimensional chiral perovskites even in the absence of an external magnetic field. In contrast, comparable photoluminesceence polarization could only be achieved with 3D achiral perovskites under an external magnetic field of 5 Tesla.[6] On the other hand, chiral perovskite quantum dots,[17] perovskite nanocrystals in chiral organic matrix,[18] and metal-free 3D chiral perovskites[19] were reported recently, and second harmonic generation was also observed in chiral perovskite nanowires.[20] These pioneering works show that low-dimensional perovskites have paved the way for chiral HOIPs as powerful optoelectronics and spintronic materials. In this study, we proposed several 3D chiral HOIPs by introducing chiral cations, which have been proved to be kinetically and thermodynamically stable.
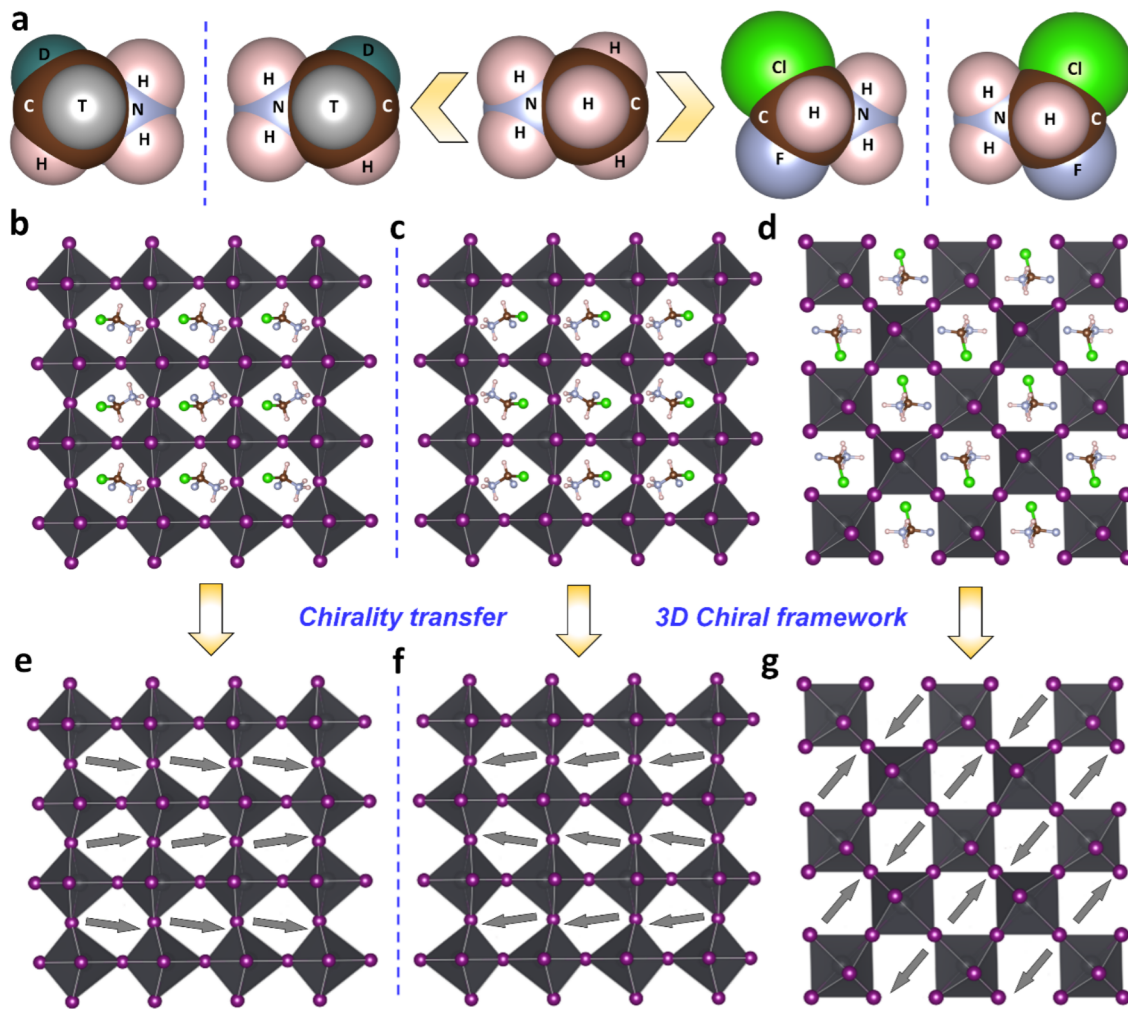
Figure 1. Structures of 3D chiral HOIPs. a) The chemical structures of methylammonium and its chiral derivatives: (R)- and (S)-deuterotritomethylammonium, (R)- and (S)-chlorofluoromethylammonium. The optimized structures of 3D chiral HOIPs, (R)-CHFClNH$_3$PbI$_3$ (b), (S)-CHFClNH$_3$PbI$_3$ (c) together with the achiral (RS)-CHFClNH$_3$PbI$_3$ (d). The framework of the optimized 3D chiral perovskite after removing chiral cations, (R)-CHFClNH$_3$PbI$_3$ (e), (S)-CHFClNH$_3$PbI$_3$ (f) together with the achiral (RS)-CHFClNH$_3$PbI$_3$ (g). The direction of the electrical dipole moment of the chiral cations in these 3D chiral HOIPs is shown in (e)-(g).

Compared to the low-dimensional counterparts, 3D HOIPs exhibit smaller exciton binding energy and much longer charge-carrier diffusion lengths,[2] making them more

promising toward applications in circularly polarized electronics, photonics and spintronics after combining with chirality. However, the design of 3D chiral HOIPs is still challenging because the cuboctahedral cavity in 3D perovskites is very small, and only small organic cations (*e.g.* methylammonium ($CH_3NH_3^+$) or formamidinium ($NH_2CHNH_2^+$)) or inorganic cations (*e.g.* Cs^+ or Rb^+) can be inserted.[21] The smallest chiral cation for 3D HOIPs is $CHDTNH_3^+$ (D=$_1^2H$, T=$_1^3H$), but the strong radioactivity of T and its short half-life belies its usefulness. Instead, we look to fluorine and chlorine, whose *Van der Waals* radii of 147 pm and 175 pm, respectively, are only slightly larger than that of hydrogen (120 pm). Thus, we choose the smallest functional chiral cation: (*R*)- and (*S*)-chlorofluoromethylammonium (as shown in **Figure 1**a), along with the corresponding 3D chiral HOIPs for further study.

As shown in **Figure 1**b-1d, we have optimized the structures of chiral (*R*)-$CHFClNH_3PbI_3$ and (*S*)-$CHFClNH_3PbI_3$, together with the achiral (*RS*)-$CHFClNH_3PbI_3$. Since we could not forecast the exact chiral space group of the proposed 3D chiral HOIPs, we have defined the chiral (*R*)-$CHFClNH_3PbI_3$ and (*S*)-$CHFClNH_3PbI_3$ into the simplest **$P2$** chiral space group, while (*RS*)-$CHFClNH_3PbI_3$ was built into the **$P\overline{1}$** centrosymmetric space group.

The structures of the 3D chiral perovskites were optimized by Vienna *ab initio* simulation package (VASP),[22] which implements the projected augmented wave (PAW) approach.[23] The exchange correlation was calculated by the Perdew-Burke-Ernzerhof (PBE) functional,[24] and the energy cutoff was set as 400 eV. DFT-D2 method of Grimme was employed to describe the *Van der Waals* interactions.[25] The geometric structures of these 3D chiral perovskites were optimized until the force on every atom was smaller than 0.001 eV/Å. Intriguingly, the chiral space group and the octahedral structure of these chiral perovskites still maintain during the structure relaxation. The optimized cell parameters are summarized in Table S1. The Pb-I bond length in (*R*)-$CHFClNH_3PbI_3$ is in the range of 3.003 Å and 3.399 Å,

slightly longer than the Pb-I bond length of 3.196 Å in $CH_3NH_3PbI_3$,[26] which we attribute to the increased volume of the chiral cation.

We then looked to confirm whether the chirality is successfully transferred from the chiral cations to the framework of the 3D HOIPs. After removing the chiral cations (as shown in **Figure 1**e-1g), we re-defined the space group of the 3D PbI_6^{4-} framework; the chiral space group of **P2** still maintains, indicating the successful chirality transfer. As shown in **Figure 1**e and **1**f, the electrical dipole moments of the chiral cations in (R)-$CHFClNH_3PbI_3$ and (S)-$CHFClNH_3PbI_3$ point to the opposite direction, owing to their enantiomeric nature. However, the situation in (RS)-$CHFClNH_3PbI_3$ differs. The electrical dipole moments of the neighboring chiral cations adopt an anti-parallel arrangement, and the total polarization is zero, consistent with the centrosymmetric structure of the achiral (RS)-$CHFClNH_3PbI_3$.
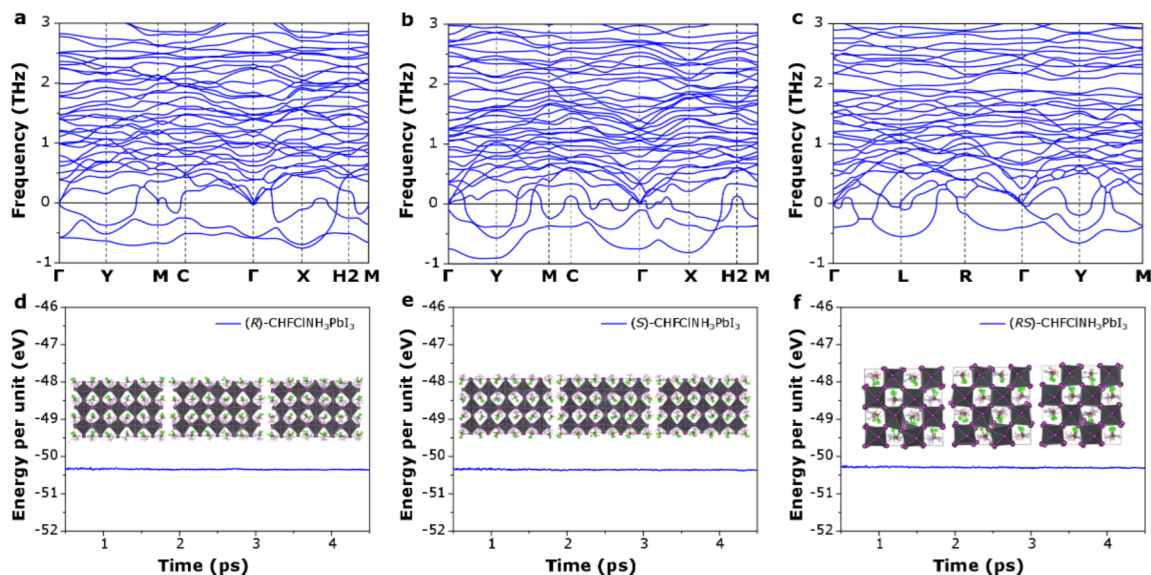
Figure 2. The thermodynamic and kinetic stability of the 3D chiral HOIPs. The phonon spectra of (R)-$CHFClNH_3PbI_3$ (a), (S)-$CHFClNH_3PbI_3$ (b) and (RS)-$CHFClNH_3PbI_3$ (c) at 300 K. The energy fluctuation of (R)-$CHFClNH_3PbI_3$ (d), (S)-$CHFClNH_3PbI_3$ (e) and (RS)-$CHFClNH_3PbI_3$ (f) supercells in *ab initio* molecular dynamics simulations.

The thermodynamic and kinetic stability of these 3D chiral HOIPs were then investigated. To assess thermodynamic stability, we have calculated the formation energies ($E_{formation}$) and dissociation energies ($E_{dissociation}$), together with the phonon spectra of these 3D chiral perovskites at 300 K. The formation energy and dissociation energy is with respect to the atomic constituents (**Equation 1**) and solid constituents (**Equation 2**) here,

$$E_{formation} = E_{Perovskite} - E_{graphite} - \frac{1}{2}E_{H_2} - \frac{1}{2}E_{F_2} - \frac{1}{2}E_{Cl_2} - \frac{1}{2}E_{N_2} - E_{Pb} - \frac{3}{2}E_{I_2} \quad \textbf{Equation 1}$$

$$E_{dissociation} = E_{PbI_2} + E_{CHFClNH_2} + E_{HI} - E_{Perovskite} \qquad \textbf{Equation 2}$$

where $E_{perovskite}$, E_{PbI_2}, E_{Pb} and $E_{graphite}$ are the energies of 3D chiral perovskite, lead (II) iodide, lead and graphite, respectively. E_{H_2}, E_{F_2}, E_{Cl_2}, E_{N_2}, E_{I_2}, $E_{CHFClNH_2}$ and E_{HI} are isolated H_2, F_2, Cl_2, N_2, I_2, $CHFClNH_2$ and HI molecules respectively.

As shown in Table S2, all 3D chiral perovskites exhibit negative formation energies and positive dissociation energies close to $CH_3NH_3PbI_3$, which confirms that 3D chiral HOIPs are thermodynamically stable at 300 K. We then calculated the phonon frequencies at 300 K based on a sampling mesh in reciprocal space by Temperature Dependent Effective Potential (TDEP 1.1).[27] Such a method employs *ab initio* molecular dynamics simulations and provides a consistent and easier computational way to extract the best possible harmonic or higher order potential energy surface, together with the lattice dynamics and thermodynamic properties of the investigated system at finite temperatures. It was found that the second-order terms are sufficient to accurately describe the systems where the anharmonic effects are known to be prevalent.[27b] As shown in **Figure 2**a-**2**c, only very small imaginary modes (< 1 THz) are found in the 3D chiral HOIPs at 300 K, suggesting that 3D HOIPs are thermodynamically stable. These small imaginary modes are a very common feature for the perovskite structures[28] and has been confirmed by both experiments (*e.g.*, $CH_3NH_3PbBr_3$)[29] and theoretical calculations

(*e.g.*, cubic phase $CH_3NH_3PbI_3$).[30] The origin of imaginary frequencies may be potentially due to the anharmonicity,[30-31] which was caused by the rotations and tiling of the octahedral.[28, 32]

For kinetic stability, we used *ab initio* molecular dynamics (AIMD) simulations.[33] The AIMD simulations were carried out under canonical *NVT* ensemble at 300 K for 4.5 ps with a time step of 0.5 fs in supercells with the lattice constant larger than 17.5 Å. As shown in **Figure 2**d-**2**f, all structures reached dynamic stable states after 0.5 ps. While the temperature and total energy fluctuates with time, the inorganic 3D PbI_6^{4-} framework still maintains. The rotation of chiral cations distorts the inorganic frameworks within only a small amplitude, and no ion migration is observed. Therefore, based on the above-optimized structures, formation energies, together with the phonon spectra and AIMD simulations, we affirm that these 3D chiral and achiral HOIPs should be both kinetically and thermodynamically stable.
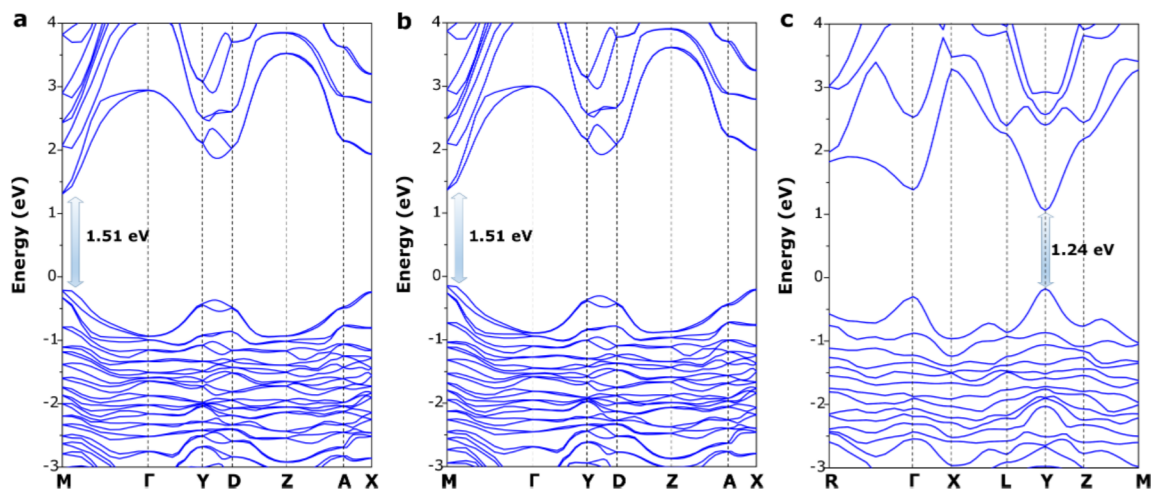

Figure 3. The calculated band structures of the 3D chiral HOIPs based on the HSE06 functional: a) (*R*)-$CHFClNH_3PbI_3$, b) (*S*)-$CHFClNH_3PbI_3$ and c) achiral (*RS*)-$CHFClNH_3PbI_3$.

The electronic structures of the 3D chiral HOIPs were investigated based on the screened hybrid Heyd-Scu-seria-Ernzerhof 2006 (HSE06) functional[34] together with spin-orbital couplings (SOC). The Brillouin zone samplings were done with Γ-centered 9×9×9 Monkhorst-Pack k points mesh. As shown in **Figure 3**, the 3D chiral HOIPs exhibit direct

bandgaps, and the enantiomer (R)-CHFClNH$_3$PbI$_3$ and (S)-CHFClNH$_3$PbI$_3$ exhibit similar band structure. The bandgap for achiral (RS)-CHFClNH$_3$PbI$_3$ is 1.24 eV, which is slightly lower than that of 1.51 eV for chiral (R)-CHFClNH$_3$PbI$_3$ and (S)-CHFClNH$_3$PbI$_3$. The reciprocal space of (R)-CHFClNH$_3$PbI$_3$ and (S)-CHFClNH$_3$PbI$_3$ is identical, hence the band structures and phonon spectra are similar. The unit cell of (RS)-CHFClNH$_3$PbI$_3$ is actually a $1/2 \times \sqrt{2} \times \sqrt{2}$ super cell of (R)-CHFClNH$_3$PbI$_3$ or (S)-CHFClNH$_3$PbI$_3$. Hence, the reciprocal space of (RS)-CHFClNH$_3$PbI$_3$ differs from (R)-CHFClNH$_3$PbI$_3$ and (S)-CHFClNH$_3$PbI$_3$. This leads to different shape of phonon spectra and band structures. The absorption spectra of the 3D chiral perovskites were then calculated and shown in Figure S1. Consistent with the above band structures, (R)-CHFClNH$_3$PbI$_3$ and (S)-CHFClNH$_3$PbI$_3$ exhibit the similar absorption spectra, while which is different for (RS)-CHFClNH$_3$PbI$_3$.

In addition, the projected density of states (PDOS) of these 3D chiral HOIPs demonstrate that beside Pb and I (as shown in Figure S2), chiral cations also contribute to the valence band and conduction band of the perovskites. As shown in **Figure 4**, we have plotted the isosurface of the self-consistent electron density (isovalue=0.0005) of the conduction band minimum (CBM) and valence band maximum (VBM) of (R)-CHFClNH$_3$PbI$_3$, (S)-CHFClNH$_3$PbI$_3$ and (RS)-CHFClNH$_3$PbI$_3$, respectively. Consistent with the reported lead halide perovskite materials,[35] the CBM of 3D chiral perovskite is also made up of an empty Pb $6p$ orbital, and VBM is made up of Pb $6s$ and I $5p$ orbitals. Most importantly, the contribution of electronegative fluorine and chlorine atoms to the VBM and CBM could also be clearly visualized. This further supports the idea that chiral cations indeed influence the optical and electronic properties of the 3D chiral HOIPs.[36]
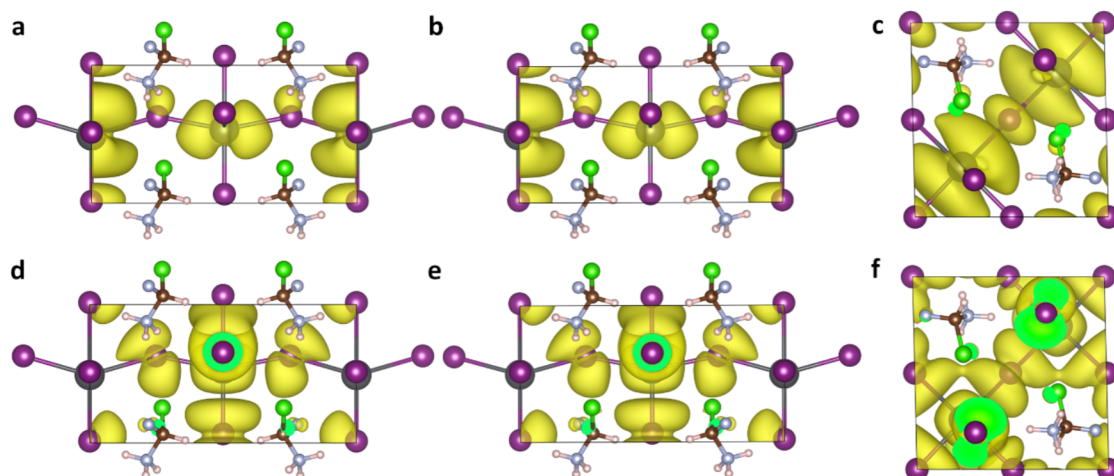
Figure 4. Isosurface plot of the self-consistent electron density (isovalue=0.0005) of the conduction band minimum (a, b, c) and valence band maximum (d, e, f) of (R)-CHFClNH$_3$PbI$_3$ and (S)-CHFClNH$_3$PbI$_3$ and (RS)-CHFClNH$_3$PbI$_3$, respectively.

From the relationship between the physical properties and point group of non-centrosymmetric single crystals (a.k.a. Neumann-Curie principle[1a, b]), these 3D chiral HOIPs should have intrinsic properties such as optical rotation, circular dichroism, second-harmonic generation, piezoelectricity, pyroelectricity and ferroelectricity (as shown in Figure S3).[19, 37]

In summary, we have confirmed that 3D chiral HOIPs are both thermodynamically and kinetically stable through structural optimization, formation energy, phonon spectra and *ab initio* molecular dynamics simulations. Combining chirality with the impressive optical, electrical and spintronic properties of 3D perovskites, 3D chiral HOIPs would be of great significance in the production of circularly polarized perovskite light-emitting diodes, waveguides, photodetectors, lasers, single photon light sources, X/γ-ray detectors, spintronics and topological quantum optics.

Experimental Section

All calculations including AIMD simulations, were carried out by Vienna *ab initio* simulation package[22], which implements the projected augmented wave approach.[23] The PAW potential with valance electrons of $1s^1$ (H), $2s^2 2p^2$ (C), $2s^2 2p^3$ (N), $2s^2 2p^5$ (F), $3s^2 3p^5$ (Cl), $5s^2 5p^5$ (I) and $5d^{10} 6s^2 6p^2$ (Pb) are used. The exchange correlation was calculated by the Perdew-Burke-Ernzerhof functional.[24] As *Van der Waals* interaction has been shown important influence on structure optimization, the DFT-D2 method of Grimme was also implemented.[25] Geometric structures were relaxed until the force on every atom was smaller than 0.001 eV/Å. The cutoff energy was 400 eV for structure relaxations and AIMD simulations. Γ-centered 9×9×9 Monkhorst-Pack mesh k points were used to calculate density of states (DOS) and band structures. For band structures, 40 points were inserted between every two high-symmetry k points with cut-off energy of 550 eV. In order to obtain more accurate electronic structures, HSE06+SOC have been implemented to calculate the band structures. The temperature dependent phonon spectra are calculated based on the last 1.5 ps of AIMD simulations by Temperature Dependent Effective Potential (TDEP 1.1),[27] which implemented advanced methods that can use the second-order force constant to accurately describe the systems where the anharmonic effects are known to be prevalent.[27] Supercells with size of 24.7 Å × 19.2 Å ×18.6 Å for (*R*)-CHFClNH$_3$PbI$_3$ and (*S*)-CHFClNH$_3$PbI$_3$, and 18.7 Å × 17.6 Å × 17.9 Å for (*RS*)-CHFClNH$_3$PbI$_3$ with Gamma point were used to perform AIMD simulations with time step of 0.5 fs.

Supporting Information
Supporting Information is available from the Wiley Online Library or from the author.

References

[1] a) F. E. Neumann and O. E. Meyer, *Vorlesungen über die Theorie der Elasticität der festen Körper und des Lichtäthers, gehalten an der Universität Königsberg*, B. G. Teubner, Leipzig, **1885**, p. xiii, 374 p; b) P. Curie, *J. Phys. Theor. Appl.* **1894**, *3*, 393-415; c) P.-P. Shi, Y.-Y. Tang, P.-F. Li, W.-Q. Liao, Z.-X. Wang, Q. Ye and R.-G. Xiong, *Chem. Soc. Rev.* **2016**, *45*, 3811-3827.

[2] a) S. D. Stranks, G. E. Eperon, G. Grancini, C. Menelaou, M. J. P. Alcocer, T. Leijtens, L. M. Herz, A. Petrozza and H. J. Snaith, *Science* **2013**, *342*, 341-344; b) G. Xing, N. Mathews, S. Sun, S. S. Lim, Y. M. Lam, M. Grätzel, S. Mhaisalkar and T. C. Sum, *Science* **2013**, *342*, 344-347.

[3] E. J. Juarez-Perez, R. S. Sanchez, L. Badia, G. Garcia-Belmonte, Y. S. Kang, I. Mora-Sero and J. Bisquert, *J. Phys. Chem. Lett.* **2014**, *5*, 2390-2394.

[4] D. Shi, V. Adinolfi, R. Comin, M. Yuan, E. Alarousu, A. Buin, Y. Chen, S. Hoogland, A. Rothenberger, K. Katsiev, Y. Losovyj, X. Zhang, P. A. Dowben, O. F. Mohammed, E. H. Sargent and O. M. Bakr, *Science* **2015**, *347*, 519-522.

[5] a) H. Zhu, Y. Fu, F. Meng, X. Wu, Z. Gong, Q. Ding, M. V. Gustafsson, M. T. Trinh, S. Jin and X. Y. Zhu, *Nat. Mater.* **2015**, *14*, 636; b) G. Xing, N. Mathews, S. S. Lim, N. Yantara, X. Liu, D. Sabba, M. Grätzel, S. Mhaisalkar and T. C. Sum, *Nat. Mater.* **2014**, *13*, 476.

[6] C. Zhang, D. Sun, C. X. Sheng, Y. X. Zhai, K. Mielczarek, A. Zakhidov and Z. V. Vardeny, *Nat. Phys.* **2015**, *11*, 427.

[7] Y. Liu, L. Collins, R. Proksch, S. Kim, B. R. Watson, B. Doughty, T. R. Calhoun, M. Ahmadi, A. V. Ievlev, S. Jesse, S. T. Retterer, A. Belianinov, K. Xiao, J. Huang, B. G. Sumpter, S. V. Kalinin, B. Hu and O. S. Ovchinnikova, *Nat. Mater.* **2018**, *17*, 1013-1019.

[8] D. Niesner, M. Wilhelm, I. Levchuk, A. Osvet, S. Shrestha, M. Batentschuk, C. Brabec and T. Fauster, *Phys. Rev. Lett.* **2016**, *117*, 126401.

[9] a) N. J. Jeon, H. Na, E. H. Jung, T.-Y. Yang, Y. G. Lee, G. Kim, H.-W. Shin, S. Il Seok, J. Lee and J. Seo, *Nat. Energy* **2018**, *3*, 682-689; b) H. Tsai, W. Nie, J.-C. Blancon, C. C. Stoumpos, R. Asadpour, B. Harutyunyan, A. J. Neukirch, R. Verduzco, J. J. Crochet, S. Tretiak, L. Pedesseau, J. Even, M. A. Alam, G. Gupta, J. Lou, P. M. Ajayan, M. J. Bedzyk, M. G. Kanatzidis and A. D. Mohite, *Nature* **2016**, *536*, 312; c) D. Bi, C. Yi, J. Luo, J.-D. Décoppet, F. Zhang, Shaik M. Zakeeruddin, X. Li, A. Hagfeldt and M. Grätzel, *Nat. Energy* **2016**, *1*, 16142; d) G. E. Eperon, T. Leijtens, K. A. Bush, R. Prasanna, T. Green, J. T. W. Wang, D. P. McMeekin, G. Volonakis, R. L. Milot, R. May, A. Palmstrom, D. J. Slotcavage, R. A. Belisle, J. B. Patel, E. S. Parrott, R. J. Sutton, W. Ma, F. Moghadam, B. Conings, A. Babayigit, H. G. Boyen, S. Bent, F. Giustino, L. M. Herz, M. B. Johnston, M. D. McGehee and H. J. Snaith, *Science* **2016**, *354*, 861-865; e) Y. Zhou and G. Long, *J. Phys. Chem. C* **2017**, *121*, 1455-1462.

[10] a) M. Yuan, L. N. Quan, R. Comin, G. Walters, R. Sabatini, O. Voznyy, S. Hoogland, Y. Zhao, E. M. Beauregard, P. Kanjanaboos, Z. Lu, D. H. Kim and E. H. Sargent, *Nat. Nanotech.* **2016**, *11*, 872; b) N. Wang, L. Cheng, R. Ge, S. Zhang, Y. Miao, W. Zou, C. Yi, Y. Sun, Y. Cao, R. Yang, Y. Wei, Q. Guo, Y. Ke, M. Yu, Y. Jin, Y. Liu, Q. Ding, D. Di, L. Yang, G. Xing, H. Tian, C. Jin, F. Gao, R. H. Friend, J. Wang and W. Huang, *Nat. Photon.* **2016**, *10*, 699.

[11] Y. Jia, R. A. Kerner, A. J. Grede, B. P. Rand and N. C. Giebink, *Nat. Photon.* **2017**, *11*, 784-788.

[12] a) H. Wei, Y. Fang, P. Mulligan, W. Chuirazzi, H.-H. Fang, C. Wang, B. R. Ecker, Y. Gao, M. A. Loi, L. Cao and J. Huang, *Nat. Photon.* **2016**, *10*, 333; b) Q. Lin, A. Armin, P. L. Burn and P. Meredith, *Nat. Photon.* **2015**, *9*, 687.

[13] J. Wang, C. Zhang, H. Liu, R. McLaughlin, Y. Zhai, S. R. Vardeny, X. Liu, S. McGill, D. Semenov, H. Guo, R. Tsuchikawa, V. V. Deshpande, D. Sun and Z. V. Vardeny, *Nat. Commun.* **2019**, *10*, 129.

[14] D. G. Billing and A. Lemmerer, *Acta Cryst. Sect. E* **2003**, *59*, m381-m383.

[15] D. G. Billing and A. Lemmerer, *CrystEngComm* **2006**, *8*, 686-695.

[16] G. Long, C. Jiang, R. Sabatini, Z. Yang, M. Wei, L. N. Quan, Q. Liang, A. Rasmita, M. Askerka, G. Walters, X. Gong, J. Xing, X. Wen, R. Quintero-Bermudez, H. Yuan, G. Xing, X. R. Wang, D. Song, O. Voznyy, M. Zhang, S. Hoogland, W. Gao, Q. Xiong and E. H. Sargent, *Nat. Photon.* **2018**, *12*, 528-533.

[17] Z. N. Georgieva, B. P. Bloom, S. Ghosh and D. H. Waldeck, *Adv. Mater.* **2018**, *30*, 1800097.

[18] Y. Shi, P. Duan, S. Huo, Y. Li and M. Liu, *Adv. Mater.* **2018**, *30*, 1705011.

[19] H.-Y. Ye, Y.-Y. Tang, P.-F. Li, W.-Q. Liao, J.-X. Gao, X.-N. Hua, H. Cai, P.-P. Shi, Y.-M. You and R.-G. Xiong, *Science* **2018**, *361*, 151-155.

[20] C. Yuan, X. Li, S. Semin, Y. Feng, T. Rasing and J. Xu, *Nano Lett.* **2018**, *18*, 5411-5417.

[21] a) X. Meng, R. Zhang, Z. Fu and Q. Zhang, *Phys. Chem. Chem. Phys.* **2016**, *18*, 27358-27365; b) A. Jain, O. Voznyy and E. H. Sargent, *J. Phys. Chem. C* **2017**, *121*, 7183-7187; c) M. Becker, T. Klüner and M. Wark, *Dalton Trans.* **2017**, *46*, 3500-3509; d) S. Körbel, M. A. L. Marques and S. Botti, *J. Mater. Chem. C* **2016**, *4*, 3157-3167; e) C. Kim, T. D. Huan, S. Krishnan and R. Ramprasad, *Sci. Data* **2017**, *4*, 170057.

[22] a) G. Kresse and J. Furthmüller, *Comp. Mater. Sci.* **1996**, *6*, 15-50; b) G. Kresse and J. Hafner, *J. Phys. Condens. Matter* **1994**, *6*, 8245.

[23] P. E. Blöchl, *Phys. Rev. B* **1994**, *50*, 17953-17979.

[24] J. P. Perdew, A. Ruzsinszky, G. I. Csonka, O. A. Vydrov, G. E. Scuseria, L. A. Constantin, X. Zhou and K. Burke, *Phys. Rev. Lett.* **2008**, *100*, 136406.

[25] S. Grimme, *J. Comput. Chem.* **2006**, *27*, 1787-1799.

[26] C. C. Stoumpos, C. D. Malliakas and M. G. Kanatzidis, *Inorg. Chem.* **2013**, *52*, 9019-9038.

[27] a) L. Chaput, A. Togo, I. Tanaka and G. Hug, *Phys. Rev. B* **2011**, *84*, 094302; b) O. Hellman, I. A. Abrikosov and S. I. Simak, *Phys. Rev. B* **2011**, *84*, 180301.

[28] N. A. Benedek and C. J. Fennie, *J.Phys.Chem.C* **2013**, *117*, 13339-13349.

[29] I. P. Swainson, C. Stock, S. F. Parker, L. Van Eijck, M. Russina and J. W. Taylor, *Phys. Rev. B* **2015**, *92*, 100303.

[30] F. Brivio, J. M. Frost, J. M. Skelton, A. J. Jackson, O. J. Weber, M. T. Weller, A. R. Goñi, A. M. A. Leguy, P. R. F. Barnes and A. Walsh, *Phys. Rev. B* **2015**, *92*, 144308.

[31] a) A. M. A. Leguy, A. R. Goñi, J. M. Frost, J. Skelton, F. Brivio, X. Rodríguez-Martínez, O. J. Weber, A. Pallipurath, M. I. Alonso, M. Campoy-Quiles, M. T. Weller, J. Nelson, A. Walsh and P. R. F. Barnes, *Phys. Chem. Chem. Phys.* **2016**, *18*, 27051-27066; b) K. Wang, Z. Liang, X. Wang and X. Cui, *Adv. Electron. Mater.* **2015**, *1*, 1500089; c) X.-G. Zhao, J.-H. Yang, Y. Fu, D. Yang, Q. Xu, L. Yu, S.-H. Wei and L. Zhang, *J. Am. Chem. Soc.* **2017**, *139*, 2630-2638; d) A. Marronnier, G. Roma, S. Boyer-Richard, L. Pedesseau, J.-M. Jancu, Y. Bonnassieux, C. Katan, C. C. Stoumpos, M. G. Kanatzidis and J. Even, *ACS Nano* **2018**, *12*, 3477-3486.

[32] A. N. Beecher, O. E. Semonin, J. M. Skelton, J. M. Frost, M. W. Terban, H. Zhai, A. Alatas, J. S. Owen, A. Walsh and S. J. L. Billinge, *ACS Energy Lett.* **2016**, *1*, 880-887.

[33] a) M.-G. Ju, J. Dai, L. Ma and X. C. Zeng, *Adv. Energy Mater.* **2017**, *7*, 1700216; b) S. Lu, Q. Zhou, Y. Ouyang, Y. Guo, Q. Li and J. Wang, *Nat. Commun.* **2018**, *9*, 3405.

[34] J. Heyd, G. E. Scuseria and M. Ernzerhof, *J. Chem. Phys.* **2006**, *124*, 219906.

[35] F. Brivio, A. B. Walker and A. Walsh, *APL Mater.* **2013**, *1*, 042111.

[36] a) W. Meng, X. Wang, Z. Xiao, J. Wang, D. B. Mitzi and Y. Yan, *J. Phys. Chem. Lett.* **2017**, *8*, 2999-3007; b) W.-J. Yin, J.-H. Yang, J. Kang, Y. Yan and S.-H. Wei, *J. Mater. Chem. A* **2015**, *3*, 8926-8942.

[37] a) Y.-M. You, W.-Q. Liao, D. Zhao, H.-Y. Ye, Y. Zhang, Q. Zhou, X. Niu, J. Wang, P.-F. Li, D.-W. Fu, Z. Wang, S. Gao, K. Yang, J.-M. Liu, J. Li, Y. Yan and R.-G. Xiong, *Science* **2017**, *357*, 306-309; b) W.-Q. Liao, Y.-Y. Tang, P.-F. Li, Y.-M. You and R.-G. Xiong, *J. Am. Chem. Soc.* **2017**, *139*, 18071-18077.

The table of contents entry
Three-dimensional chiral hybrid organic-inorganic perovskites are both kinetically and thermodynamically stable based on theoretical calculation, and chirality is transferred from chiral cations to the perovskite framework, which would be of great interest to the field of piezoelectricity, thermoelectricity, ferroelectricity, topological quantum optics, circularly polarized optoelectronics and spintronics.

Keyword 3D chiral perovskite, chirality transfer, circularly polarized optoelectronics, theoretical calculation

G. Long,* Y. Zhou, M. Zhang, R. Sabatini, A. Rasmita, L. Huang, G. Lakhwani, W. Gao*

Theoretical prediction of chiral three-dimensional hybrid organic-inorganic perovskites

ToC figure

3D Chiral Hybrid Organic-Inorganic Perovskites